CHAPTER 5

EJECTOR PERFORMANCE AND VALIDATION OF CFD's RESULT

In this chapter, actual performances of the experimental steam ejector were presented and discussed. Effect of four interested parameters were investigated : the condenser saturation pressure, boiler saturation temperature (130, 140, and 150°C), evaporator saturation temperature (5, 7.5, and 10°C) and the primary nozzle's throat diameter (1.4, 1.7, and 2.0 mm). For all tests, the condenser pressure was varied until the ejector was failed to operate. The actual entrainment ratio and critical condenser pressure were compared with those obtained from CFD simulation. This ensures that the CFD model was correctly developed.

5.1 Validation of the primary fluid critical mass flow rate

Figure 5.1 and table 5.1 show the comparison of primary mass flow rate through the primary nozzle between simulated and actual value. Three primary nozzles with diameter throat 1.4, 1.7 and 2.0mm were used. The boiler saturation temperature was varied in the range between 120°C and160°C.

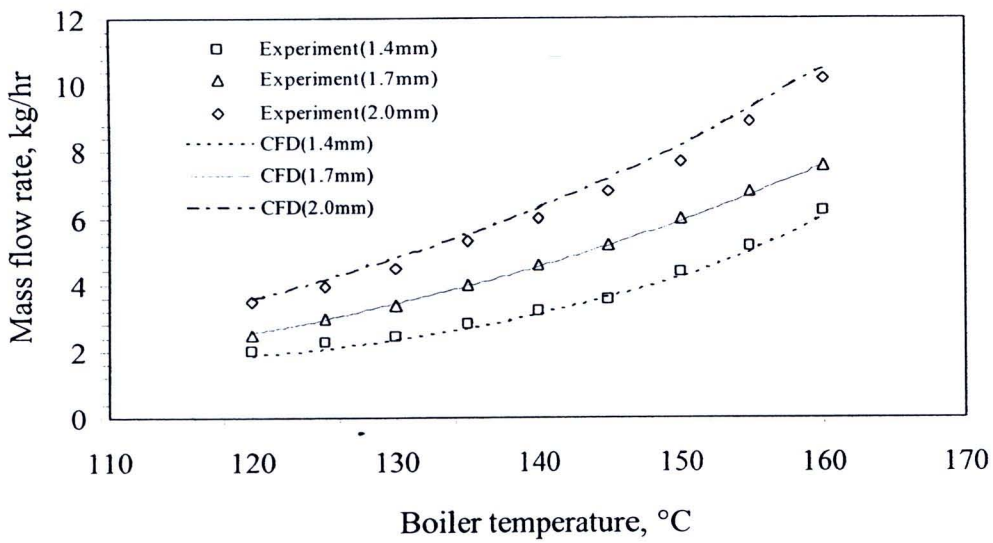

Figure 5.1: The comparison between simulated and actual result of primary fluid mass flow rate.

Table 5.1 Validation of simulated primary mass flow rate with actual result.

	Primary fluid mass flow rate (kg/hr)								
Boiler Temperature	throat 1.4mm experiment	CFD	error (%)	throat 1.7mm experiment	CFD	error (%)	throat 2.0mm experiment	CFD	error (%)
120	1.90	1.84	3.3	2.50	2.55	4.0	3.50	3.52	0.5
125	2.25	2.15	2.1	3.00	3.00	0.0	3.95	4.13	4.5
130	2.43	2.33	4.3	3.40	3.43	0.8	4.58	4.62	2.6
135	2.83	2.75	3.0	4.00	3.94	1.0	5.30	5.50	3.8
140	3.22	3.10	3.9	4.62	4.54	1.7	6.00	6.30	5.0
145	3.53	3.52	0.3	5.20	5.26	0.9	6.85	7.10	3.6
150	4.37	4.35	0.5	5.90	6.00	1.7	7.78	8.00	2.8
155	5.12	4.95	3.4	6.80	6.85	0.7	8.90	9.11	2.4
160	6.18	6.08	1.6	7.60	7.57	0.4	10.22	10.40	1.8

From the figure 5.1 and table 5.1, it can be seen that the CFD technique can be used to accurately predict the primary mass flow rate at various condition. The errors not more than 10% were found.

Referring to figure 5.1, it was found that when the boiler saturation temperature is increased, the primary nozzle allows the larger amount of primary mass flow rate through the primary nozzle. This results from the stagnation pressure and temperature of nozzle to be increased. At fixed boiler saturation temperature, as the size of primary nozzle's throat is increased, the larger amount of primary mass flow rate is also allowed through the primary nozzle. These obey the principle of supersonic compressible flow; the critical mass flow rate through the supersonic nozzle is a function of stagnation properties of the inlet fluid and cross sectional area of the nozzle's throat.

5.2 Effect of the operating pressures to the ejector performance

Figure 5.2a and 5.2b show effect of the condenser pressure to the ejector performance which are obtained experimentally and from CFD simulation. Only the primary nozzle with throat diameter of 2.0 mm (no.3) was used. The boiler and the evaporator saturation temperatures were fixed at 130°C and 7.5°C, respectively. The condenser pressure was varied until the ejector was failed to operate.

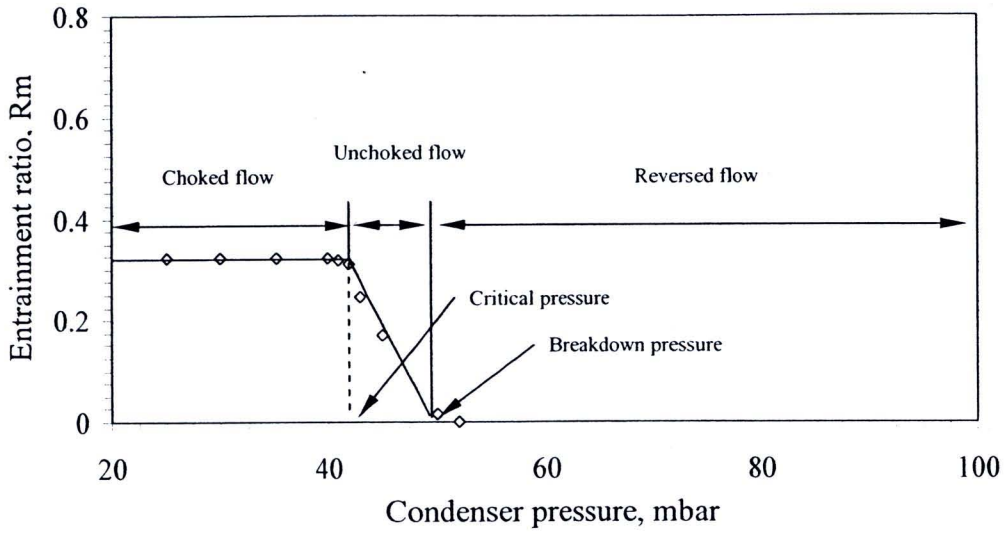

a) Smulated result (based on k-*ω-sst viscosity model*).

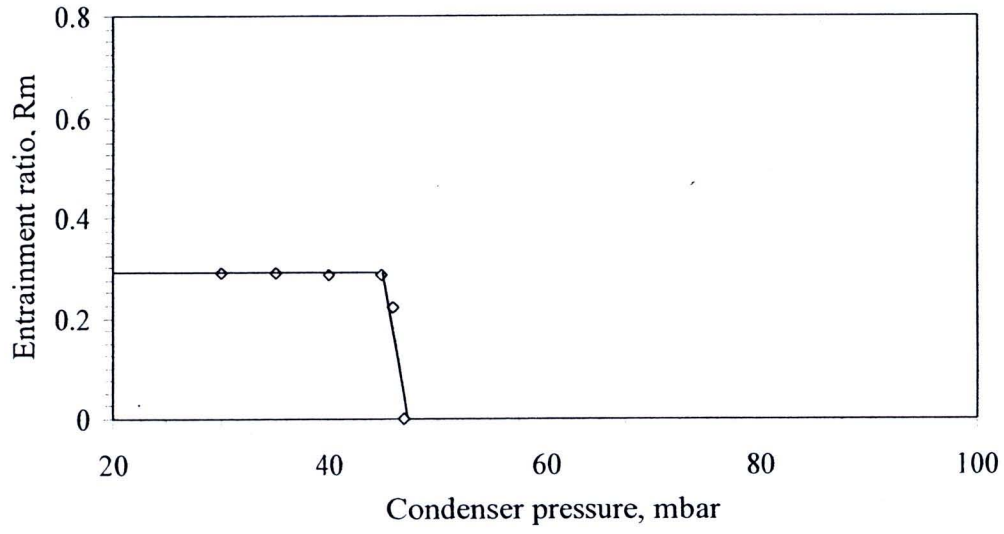

b) Experimental result.

Figure 5.2: The effect of condenser pressure.

From the figures (5.2a and 5.2b), the performance curves can be classified as three operation regions distinguished by the *critical condenser pressure* and the *breakdown condenser pressure.* They are *choked flow*, *unchoked flow*, and *reversed flow* of the secondary fluid.

In the choked flow region, where the condenser pressure is below the *critical value*, the entrainment ratio remains constant over the range of condenser pressures. Since the critical mass flow rate of the primary fluid through primary nozzle is independent from the variation of the nozzle downstream pressure (condenser and evaporator pressures). Therefore, the ejector entrains the same amount of the secondary fluid. This is because the secondary flow is choked in the mixing chamber.

In the unchoked flow region, where the condenser pressure exceeds the critical value, the entrainment ratio drops rapidly when the condenser pressure is raised. The secondary fluid is no longer choked in the mixing chamber. If the back pressure is further increased to exceed the breakdown point or operating in reversed flow region, the ejector can not entrain any secondary fluid. Moreover, the primary fluid will reverse back and causes the ejector to malfunction.

Figure 5.3a and 5.3b show effect of the boiler saturation temperature to the ejector performance which were obtained experimentally and from CFD simulation. Only the primary nozzle with throat diameter of 2.0 mm (no.3) was used. The evaporator saturation temperature was fixed at 7.5°C. Three boiler saturation temperatures were used, 130, 140, and 150°C. The condenser pressure was varied until the ejector was failed to operate.

From the figures (5.3a and 5.3b), it can be seen that, when there is an increase in the boiler saturation temperature, the ejector can be operated at a higher critical condenser pressure. However, the ejector can entrain less amount of the secondary fluid.

At a higher boiler temperature, the larger amount of the primary fluid is allowed through the primary nozzle. As a result, the primary stream will flow with a higher momentum. However, the larger amount of the primary fluid requires larger flow area in the mixing chamber which causes in a smaller flow area for the secondary fluid to be entrained. This results in a reduction in the entrainment ratio (the primary flow is increased while the secondary flow is decreased) but the ejector can be operated at a higher critical condenser pressure.

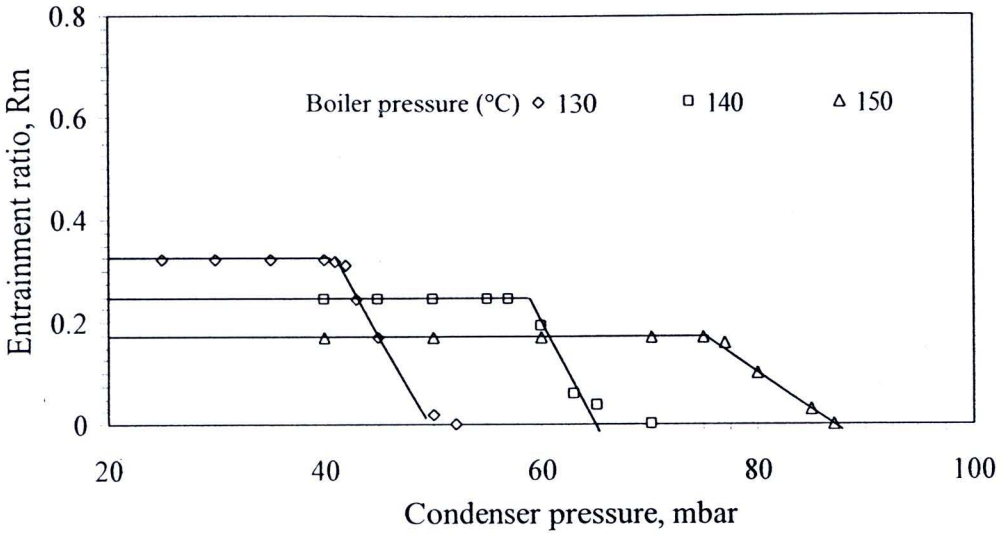

a) Simulated result (based on k-ω-*sst viscosity model*).

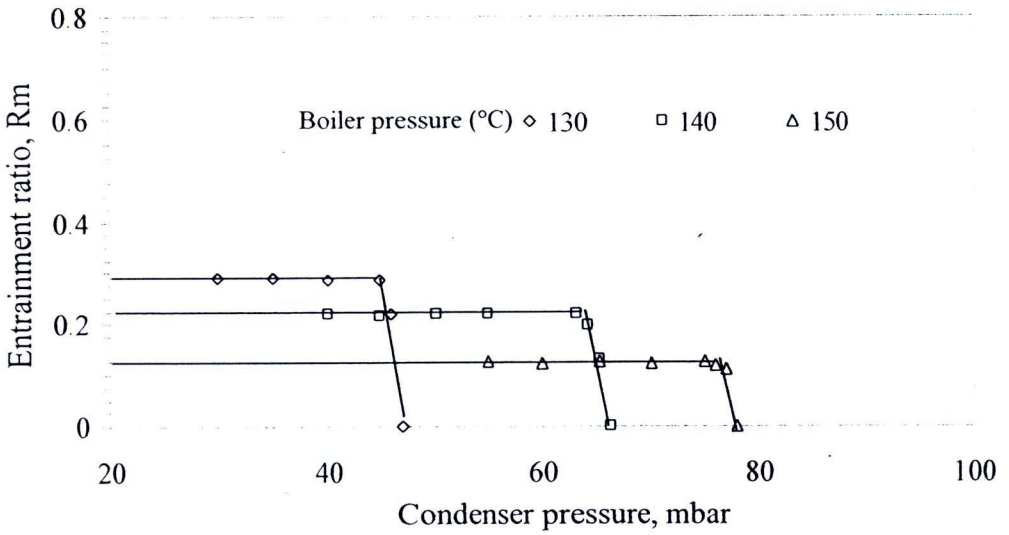

b) Experimental result.

Figure 5.3: The effect of boiler saturation temperature.

Figure 5.4a and 5.4b show effect of the evaporator saturation temperature to the ejector performance which are obtained experimentally and from CFD simulation. Only the primary nozzle with throat diameter of 2.0 mm (no.3) was used. The boiler saturation temperature was fixed at 130°C. Three evaporator saturation temperatures were used, 5°, 7.5°, and 10°C. The condenser pressure was varied until the ejector was failed to operate.

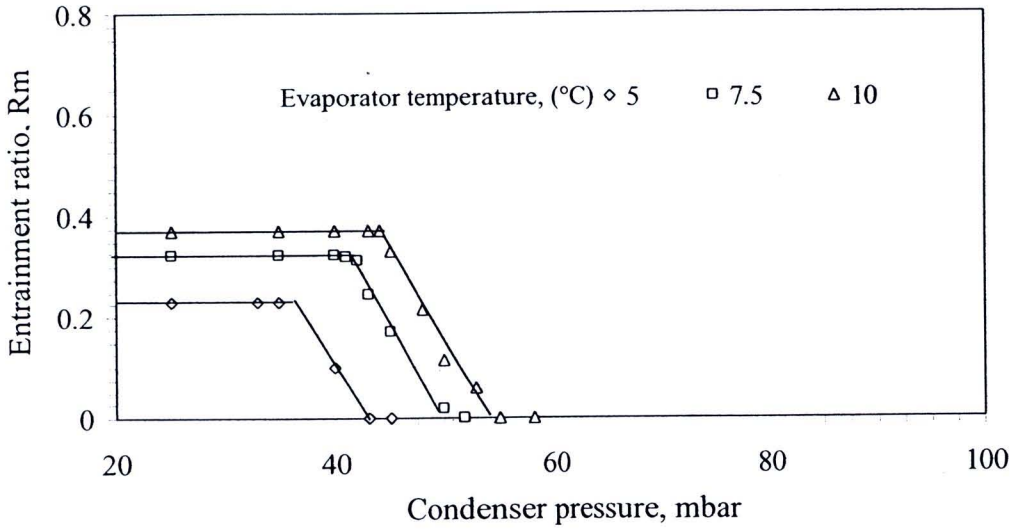

a) Simulated result (based on k-*ω-sst viscosity model*).

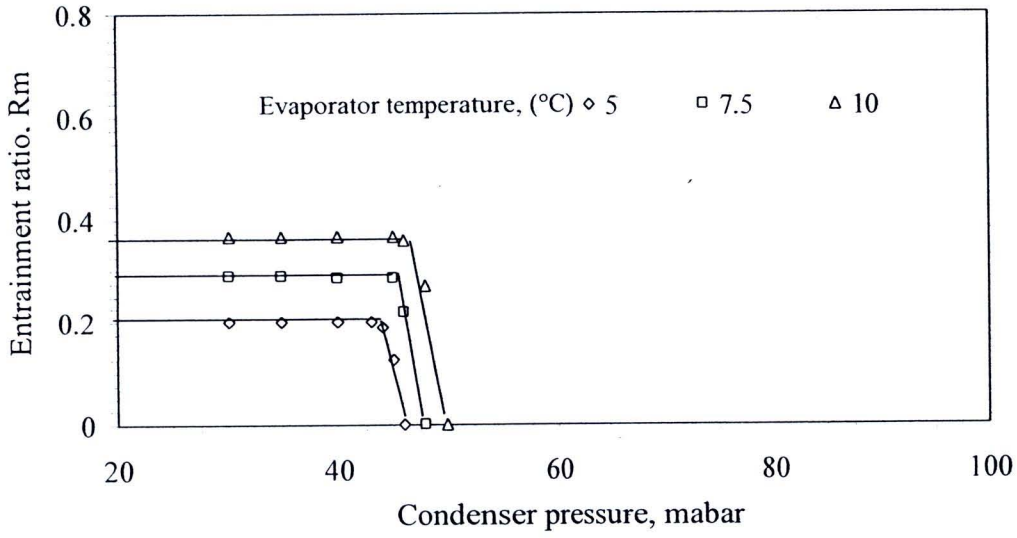

b) Experimental result.

Figure 5.4: The effect of evaporator saturation temperature.

From the figures (5.4a and 5.4b), it can be seen that, when the evaporator saturation temperature is increased, the ejector can be operated at a higher critical condenser pressure and can also entrain greater amount of the secondary fluid. The possible reason is that, the evaporator which is the upstream of the mixing chamber, when its pressure is increased, more secondary fluid is pushed into the mixing chamber while the primary fluid remains constant. Moreover, the greater amount of secondary fluid causes the total momentum of

mixed fluid to become higher, and therefore, the ejector is able to operate at a higher critical condenser pressure.

5.3 Effect of the primary nozzle's throat diameter

In this test, the boiler saturation temperature was fixed at 130°C. The evaporator saturation temperature was fixed at 7.5°C. Three primary nozzles were used. All the nozzle have equal exit to throat area ratio of 20 and should be provided the exit Mach number of 4.0 The throat diameter were of 1.0 mm (no.1), 1.7 mm (no.2), and 2.0 mm (no.3). The condenser pressure was varied until the ejector was failed to operate. The actual and simulated results were presented and compared as shown in figures 5.5a and 5.5b.

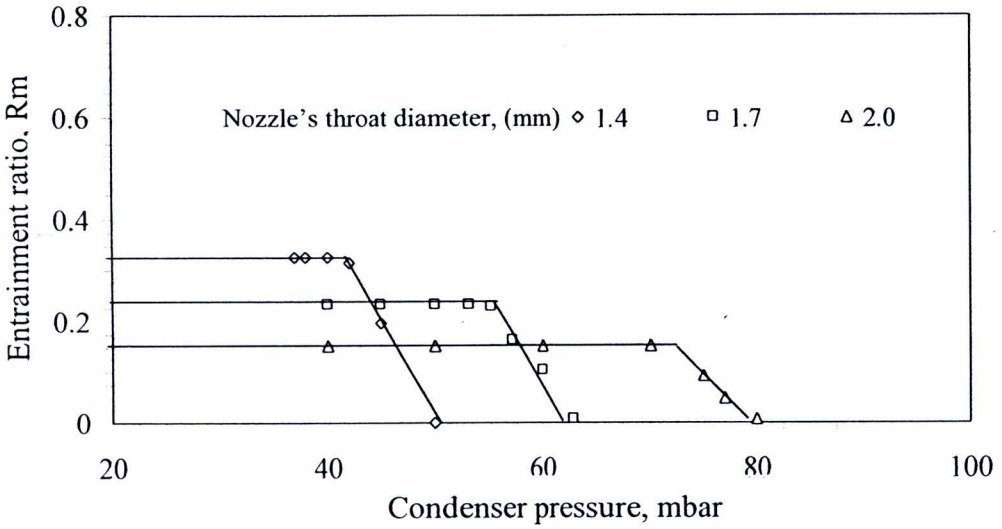

a) Simulated result (based on k-*ω-sst viscosity model*).

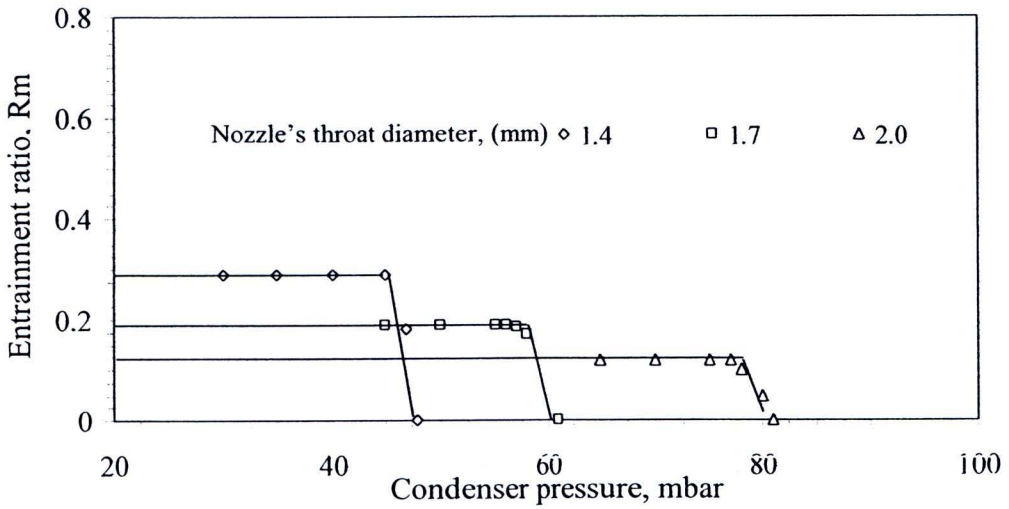

b) Experimental result.

Figure 5.5: The effect of primary nozzle's throat diameter.

From the figures (5.5a and 5.5b), it can be seen that an increase in primary nozzle's throat diameter causes the steam ejector to be able to operate at the higher critical condenser pressure. Meanwhile, the entrainment ratio is reduced when its throat area increases. The reason of reducing the entrainment ratio is that the larger size of primary nozzle's throat diameter allows the large amount of primary mass flow rate to pass through the primary nozzle. Thus, the momentum of primary flow is increased. This causes ejector to be operated at higher critical condenser pressure. However, the large amount of primary mass flow rate causes the entrainment ratio to drop. The effect of using larger nozzle is very similar to that when operating with high boiler saturation temperature.

5.4 Proficiency of CFD technique

From the previous section, FLUENT 6.3, CFD package was used to predict performance of the tested ejector. It was found the simulation results were very similar results to those obtained experimentally. In all case, the simulated entrainment ratio values were offset slightly higher and the simulated critical condenser pressure value were slightly lower than the actual values. It was also found that, the simulated results based on *k-ω-sst viscosity model* are more accurate than those based on *reliazable k-ε viscosity model.* All these results are tabulated in table 5.2.

Errors of not more than 10% were found. Possible reasons for this error may be the result of three reasons. Firstly, the working fluid properties are under the ideal gas assumption. In the actual process, even the pressure in the mixing chamber of the ejector is very low, but the fluid is very close to saturation condition. Therefore, the assumption of ideal gas may not be perfectly corrected. However, the assumption of ideal gas was selected in order to avoid the difficulty of mathematical model which results in the solution to converge to convergence criteria.

Secondly, during the simulation, the ejector's wall of physical model is set as adiabatic wall. This means that there is no heat transfer at the mixing chamber's wall boundary. However, it is impossible in order to avoid the heat transfer between the tested ejector and the surroundings.

The last reason, the condition at the wall surface of the tested ejector may not be defined exactly. In the CFD model, only smooth wall was used. However, such a smooth wall may not be possible for the tested ejector. Moreover, the primary nozzles may not be manufactured correctly since they were very small.

Regarding the simulated result based on *reliazable k-ε* and *k-ω-sst* viscosity models, it was found that the *k-ω-sst* viscosity model provided the results to be more accurate than that *reliazable k-ε* viscosity model. This was observed when the ejector was operated at a relatively high boiler temperature (higher than 140°C) or at a relatively low evaporator temperature (lower than 7.5°C). The possible reason is that the mathematical model of the *k-ω-sst* viscosity model emphasizes the free sheer flow for far wakes and mixing layer, unlike, in the case of *reliazable k-ε* viscosity model [16]. This may cause the *k-ω-sst* viscosity model to be more realistic than that *reliazable k-ε* viscosity model. Overall, it is enough to ensure that the simulated result from CFD technique is provided accurately. Moreover, it is more realistic when is investigated by the *k-ω-sst* viscosity model.

5.5 Conclusion

The study shows that the ejector's performance was strongly dependent on the operating pressure of ejector (condenser saturation pressure, boiler saturation temperature, and evaporator saturation temperature) and geometries of primary nozzle. The simulated results show the similarity in the performance curve when compared to the experimental result. The study also shows that the result provided by the *k-ω-sst* viscosity model was more realistic than that provided by *reliazable k-ε* viscosity model. However, the average errors of not more than 10% were found. Overall, it may be said that the simulated results based on CFD technique were reliable.

Table 5.2: Comparison of steam ejector's performance between simulated and actual result (at critical point).

Boiler temperature	Evaporator temperature	nozzle throat's diameter	Entrainment ratio					Critical condenser pressure				
			experiment	CFD		error[a] (%)		experiment	CFD		error[b] (%)	
				relizable k-ε	k-ω-sst	relizable k-ε	k-ω-sst		relizable k-ε	k-ω-sst	relizable k-ε	k-ω-sst
Effect of boiler saturation temperature												
130	7.5	2.0	0.29	0.32	0.31	10.3	6.9	45	42	43	6.7	7.4
140	7.5	2.0	0.22	0.24	0.23	9.1	4.5	64	60	62	6.2	3.1
150	7.5	2.0	0.13	0.17	0.14	31	7.7	77	76	76	1.3	1.3
Effect of evaporator saturation temperature												
130	5.0	2.0	0.20	0.26	0.22	30	10	43	37	46	13.9	6.9
130	7.5	2.0	0.29	0.32	0.31	10.3	6.9	45	42	43	6.7	7.4
130	10	2.0	0.36	0.37	0.37	2.8	2.8	47	44	45	6.4	4.3
Effect of nozzle's throat diameter												
150	7.5	1.4	0.29	0.37	0.22	28	10.3	45	40	42	31	6.7
150	7.5	1.7	0.19	0.25	0.21	31	10.5	57	55	55	3.5	3.5
150	7.5	2.0	0.13	0.17	0.14	31	8.3	77	76	76	1.3	1.3

[a]Error (%) = 100 × (CFD's entrainment ratio - Experiment's entrainment ratio) / Experiment's entrainment ratio.
[b]Error (%) = 100 × (CFD's critical pressure- Experiment's critical pressure) / Experiment's critical pressure.